Electronic Supplementary Material (ESI) for Catalysis Science & Technology.
This journal is © The Royal Society of Chemistry 2024

Supporting Information for

Ru Nanoclusters Supported on a Bimodal *N*, *S*-Doped Mesoporous Carbon: An Efficient and Reusable Catalyst for Selective Aerobic Oxidation of Alcohols and Amines

Mohsen Heydari,[a] Nasim Ganji,*[a] Hamzeh Hassanaki Veisi,[a] Babak Karimi,*[a,b] Hojatollah Vali[c]

[a] *Department of Chemistry, Institute for Advanced Studies in Basic Sciences (IASBS), Prof. Sobouti Boulevard, Zanjan 45137-66731, Iran*

[b] *Research Center for Basic Sciences & Modern Technologies (RBST), Institute for Advanced Studies in Basic Sciences (IASBS), Prof. Sobouti Boulevard, Zanjan 45137-66731, Iran*

[c] *Department of Anatomy and Cell Biology and Facility for Electron Microscopy Research, McGill University, Montreal, Quebec, H3A 2A7, Canada*

Table of Contents

EXPERIMENTAL SECTION

CHEMICALS

Chemicals, including poly(ethylene glycol)-block-poly(propylene glycol)-block-poly(ethylene glycol) P123 ($EO_{20}PO_{70}EO_{20}$, M_{av} = 5800), tetraethyl orthosilicate (TEOS), *n*-butanol, 1-methylimidazole, 2-bromo-1-phenylethane, guanine, sulfuric acid (98%), hydrochloric acid (37%), hydrofluoric acid (40%), $RuCl_3.xH_2O$, and all alcohols, and amines were purchased from Merck, Sigma-Aldrich, and Fluka companies. All chemicals were used without any additional purification. Toluene was dried by refluxing over sodium in the presence of benzophenone as an indicator.

CHARACTERIZATION

Nitrogen sorption analysis was carried out by a Belsorp (BELMAX, Japan) analyzer at 77 K. All samples were first degassed at 373 K for 10 h. The specific surface area of materials was calculated by the BET equation. The PSD curves were obtained using the BJH and DH methods from the adsorption and desorption branches of the isotherms, respectively. Total pore volumes were estimated using the amount of N_2 gas adsorbed at $P/P_0 \approx 0.995$. TEM images were recorded by a Philips CM-200 instrument. FT-IR analysis was performed by a Bruker vector 22 spectrometer in the 400-4000 cm^{-1} region. Raman spectrum was taken on a Bruker SENTERRA (Germany) microscope. XPS spectra were collected on a Kratos Analytical X-ray photoelectron spectrometer. TGA was carried out by a NETZSCH STA 409 PC/PG instrument (Germany) under an O_2 atmosphere (at the 25-800 °C temperature range and 10 °C/min heating rate). Elemental analysis was conducted on a Vario-EL CHNS analyzer. Ru loading of the catalysts was measured by an ICP2060P inductively coupled plasma spectrometer. Progress in the oxidation reactions was followed by a Varian CP-3800 gas chromatograph (GC) system equipped with a flame ionization detector (FID). Carbonization process was conducted using a Nabertherm LT 3/11/P330 furnace under an Ar flow.

METHODS

Synthesis of KIT-6

KIT-6 was synthesized according to the procedure reported by Kleitz *et al* [1]. Briefly, 6.0 g of Pluronic P123, 220 g of deionized water, and 12 g of HCl (37%) were poured into a round-bottom flask, and the obtained mixture was vigorously stirred for 6 h at 35 °C. Then, 6.0 g of *n*-butanol was added to the reaction flask, and the resulting mixture was stirred at 35 °C for 1 h. 12.48 g of TEOS was added to the resulting homogeneous solution at one step, and the mixture was left under stirring at 35 °C for 24 h. Next, the mixture was hydrothermally treated at 100 °C for 24 h. The white solid was filtered, washed with deionized water and ethanol several times, and dried at 100 °C. The KIT-6 material was finally obtained by removing the P123 template through the Soxhlet extraction using ethanol.

Synthesis of 1-methyl-3-phenethyl-1*H*-imidazolium hydrogen sulfate (MPIHS)

The MPIHS ionic liquid was synthesized according to the procedure previously reported by our group [2]. Typically, 1-methylimidazole (90 mmol, 7 mL), 2-bromo-1-phenylethane (100 mmol, 13.5 mL), and absolute toluene (50 mL) were poured into a round-bottom flask, and the resulting solution was refluxed under an argon atmosphere for 24 h. After cooling to room temperature, a two-phase solution consisting of 1-methyl-3-phenethyl-1H-imidazolium bromide at the bottom appeared. The ionic liquid layer was washed with absolute toluene several times and then dried under vacuum. Next, H_2SO_4 (30 mmol, 1.6 mL) was added to a solution of 1-methyl-3-phenethyl-1*H*-imidazolium bromide (30 mmol, 8gr) in dry dichloromethane (50 mL), leading to an anion-exchange process. The resulting solution was refluxed for 48 h to remove HBr produced during the reaction. Finally, the MPIHS ionic liquid was obtained after the evaporation of dichloromethane under vacuum.

Synthesis of ionic liquid-derived bimodal ordered mesoporous carbon (IBOMC)

IBOMC material was synthesized through a nanocasting procedure similar to that recently reported by our research group [3]. To do this, 2 g of MPIHS and 0.3 g of guanine (15 wt% respect to MPIHS) were added to 5 mL of a 2M HCl aqueous solution. The mixture was stirred at 100 °C until a clear solution appeared. 2 g of KIT-6 was then added to the above solution. The mixture was stirred at 100 °C for 3 h and then dried at 130 °C. The resulting orange free-flowing powder was heated at 350 °C under an argon flow. The temperature was then increased to 900 °C and kept there for 1 h to carbonize the composite. Silica template was then removed by stirring the resulting black powder in 50 mL of a 3M HF aqueous solution for 24 h. The obtained heteroatom-doped ordered mesoporous carbon was filtered, thoroughly washed with copious amount of deionized water and ethanol several times, and dried at 100 °C.

Preparation of the Ru(III)@IBOMC catalyst

50 mg of IBOMC support was ultrasonically dispersed in 15 mL of deionized water for 30 min. 3.28 mg of $RuCl_3.xH_2O$, dissolved in 5 mL of deionized water, was drop-wisely added to the well-dispersed mixture of IBOMC in water. The mixture was vigorously stirred at room temperature for 72 h. The resulting Ru(III)@IBOMC catalyst was filtered, washed with water, and dried at 100 °C. The Ru loading of the prepared catalyst was determined by ICP analysis.

Typical procedure for the aerobic oxidation of alcohols

An alcohol substrate (0.15 mmol) and Ru(III)@IBOMC (2 mol% of Ru, 12 mg) were added to a 5 mL round-bottom flask. The flask was equipped with a small magnetic bar, a condenser, and an oxygen balloon. The reaction flask was evacuated and refilled with O_2 three times. Toluene (1.5 mL) was added to the reaction mixture. The reaction mixture was stirred at 80 °C under the O_2 atmosphere for the desired reaction time. Progress of the reaction was periodically monitored by GC. After the

reaction completion, the catalyst was separated by filtration. The filtrate was diluted with ethyl acetate and, without further purification, analyzed by GC.

For recycling tests, the filtrated Ru(III)@IBOMC catalyst was washed with toluene and ethyl acetate, dried, and reused following the procedure described above.

Typical procedure for the aerobic oxidation of amines

An amine substrate (0.15 mmol) and Ru(III)@IBOMC (2 mol% of Ru, 12 mg) were added to a 5 mL round-bottom flask. The flask was equipped with a small magnetic bar, a condenser and an oxygen balloon. The reaction flask was evacuated and refilled with O_2 three times. Absolute toluene (1.5 mL) was poured into the flask. The reaction mixture was stirred at 80 °C under the O_2 atmosphere for the desired reaction time. Progress of the reaction was periodically monitored by GC. After the reaction completion, the catalyst was separated by filtration. The filtrate was diluted with ethyl acetate and, without further purification, analyzed by GC.

For recycling tests, the filtrated Ru(III)@IBOMC catalyst was washed with toluene and ethyl acetate, dried, and reused following the procedure described above.

TOF calculation method

The number of Ru atoms per nanoparticle (N) with a given diameter can be estimated using the following equation 1 [4,5].

$$N = \frac{N_A \times \rho V}{A_r} = \frac{N_A \times \rho 4\pi\, r^3}{3 \times A_r}$$

N_A = Avogadro number = 6.022×10^{23} mol^{-1}

ρ = Metal density = 12.37 $g.cm^{-3}$

A_r = Molar mass of Ru = 101.07 $g.mol^{-1}$

$d_{Average}$ = Average particle size obtained from the histogram = 1.07 nm

$$N = \frac{6.022 \times 10^{23} \times 12.37 \times 4 \times 3.14 \times (0.535 \times 10^{-7})^3}{3 \times 101.07} = 47$$

Therefore, the number of Ru atoms in a nanocluster with mean diameter of 1.07 nm can be approximated to be 47 which is between the magic-number nanocluster sizes of 13 (n=1) and 55 (n=2).

To determine the number of Ru atoms on the surface of the nanoclusters, we used the d-FE model developed by Borodzinski et al in 1997 [6]. According to this model, for a collection of metal particles of different sizes, the mean fraction of the total atoms exposed on the surface, also called as the fraction exposed (FE), is expressed as follows:

$$FE = \frac{Ns\ (Number\ of\ Surface\ atoms)}{NT\ (total\ number\ of\ metal\ atoms\ in\ nanocluster)}$$

For a given small nanocluster (d < 100 Å), the relation between the relative particle size (d_{rel}) and FE can be calculated using the following formula, proposed by Borodzinski et al:

$$drel = \frac{d}{datom} = \frac{kc}{FE^{(1/(3-Dc))}}$$

This formula is a rewritten form of the Farin-Avnir formula [7]:

$$FE = \frac{kc}{d^{(3 - Dc)}}$$

where d is the mean diameter of the nanoclusters, d_{atom} is the atomic diameter of ruthenium (0.26 nm) and D_C is a chemisorption dimension. D_C and k are constants specific to a particular shape. Coverage of a full range of nanocluster sizes can be achieved by using a different set of D_C and k_C parameters in each of two subranges, relating to small and large nanocluster sizes. These parameters are shown the following table:

D_c and k_c values for the d-FE model

Range of FE	D_C	k_C
0.01-0.2 (for large nanocluster sizes (d > 100 Å))	2.00	5.01±0.01
0.2-0.92 (for small nanocluster sizes (d < 100 Å))	2.19±0.01	3.32±0.06

Therefore,

$$drel = \frac{1.07\ nm}{0.26\ nm} = \frac{3.32}{FE^{(1/(3 - 2.19))}} = 4.11 \qquad \rightarrow FE = 0.84$$

$$Ns = FE\ \times NT = 0.84\ \times 47 \cong 40$$

FE can also be estimated for the assembly of metal particles of different sizes using the following formula [6]:

For metal particles with large sizes (d > 24.0 d_{atom}): $$FE = \frac{5.01}{drel}$$

For metal particles with small sizes (d ≤ 24.0 d_{atom}): $$FE = \frac{2.64}{(drel)^{0.81}}$$

In the case of our system, For Ru nanoclusters with $d_{average}$= 1.07 nm:

$$FE = \frac{2.64}{(4.11)^{0.81}} \cong 0.85$$

$$Ns = 0.85\ \times 47 \cong 40$$

Finally,

$$\text{For alcohol oxidation}\quad TOF = \frac{mmol\ product}{mmol\ Catalyst\ \times\ FE\ \times time}$$

$$\text{For amine oxidation}\quad TOF = 2 \times \frac{mmol\ product}{mmol\ Catalyst\ \times\ FE\ \times time}$$

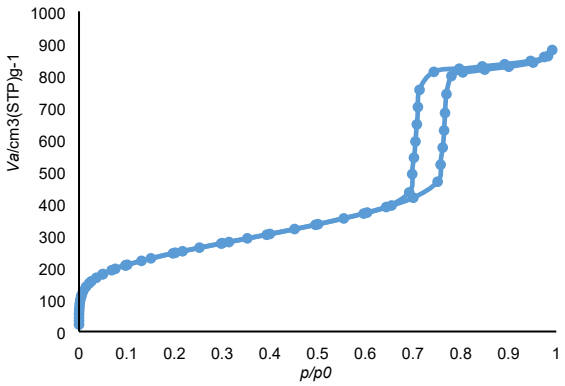

Fig. S1. N_2 adsorption-desorption isotherm of KIT-6

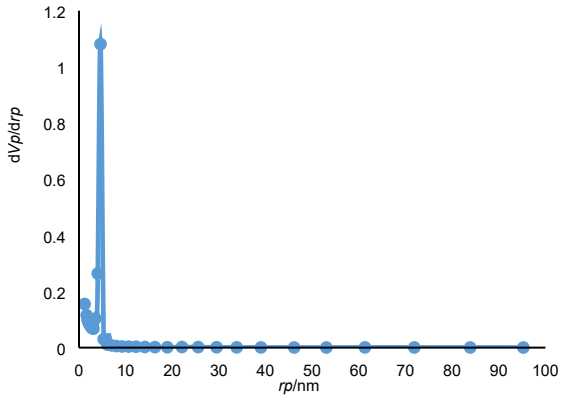

Fig. S2. Pore size distribution curve of KIT-6, evaluated using the BJH method

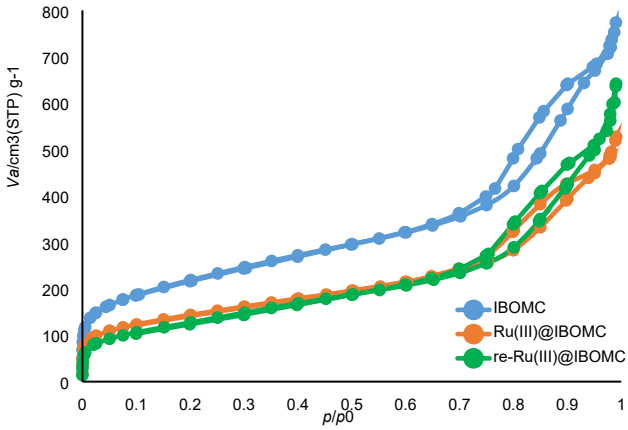

Fig. S3. N_2 adsorption-desorption isotherms of IBOMC, Ru(III)@IBOMC and re-Ru(III)@IBOMC

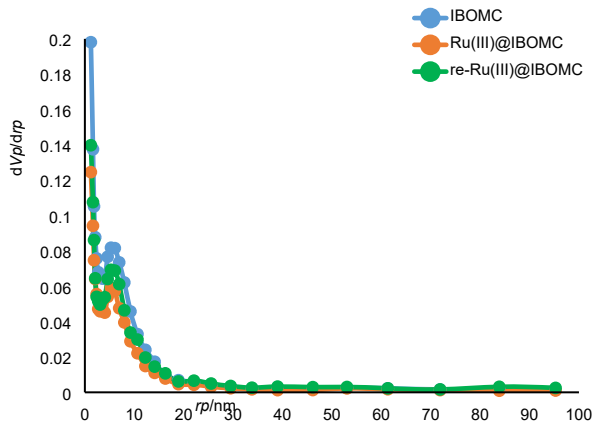

Fig. S4. BJH pore size distribution curves of IBOMC, Ru(III)@IBOMC and re-Ru(III)@IBOMC

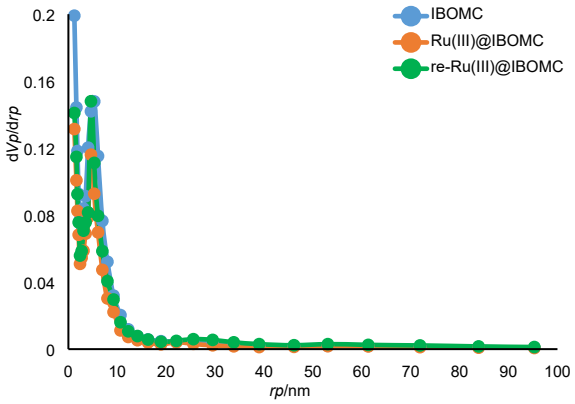

Fig. S5. DH pore size distribution curves of IBOMC, Ru(III)@IBOMC and re-Ru(III)@IBOMC

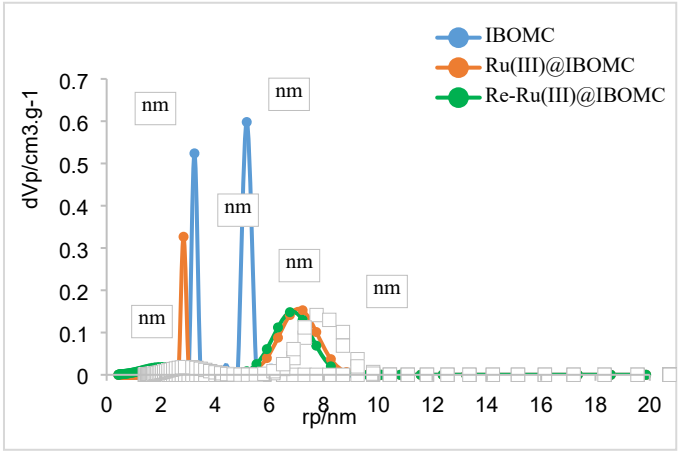

Fig. S6. NLDFT curves of IBOMC, Ru(III)@IBOMC and re-Ru(III)@IBOMC

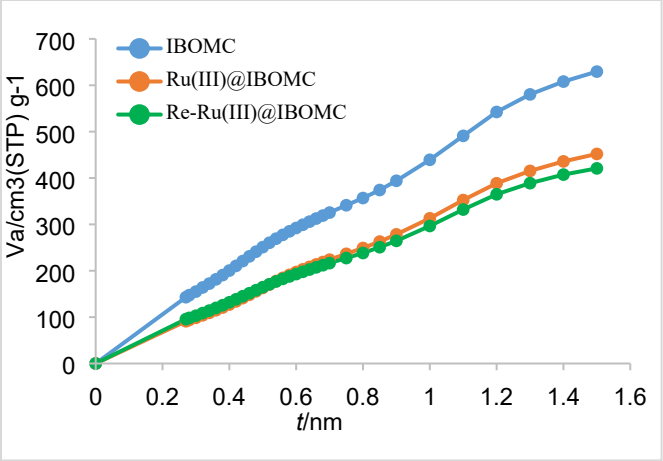

Fig. S7. *t*-plot curves of IBOMC, Ru(III)@IBOMC and re-Ru(III)@IBOMC

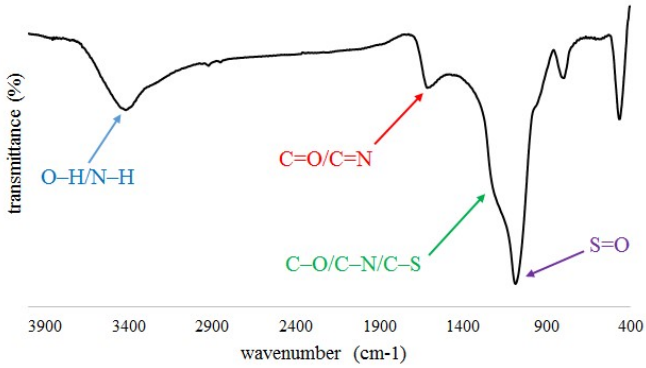

Fig. S8. FT-IR spectrum of IBOMC

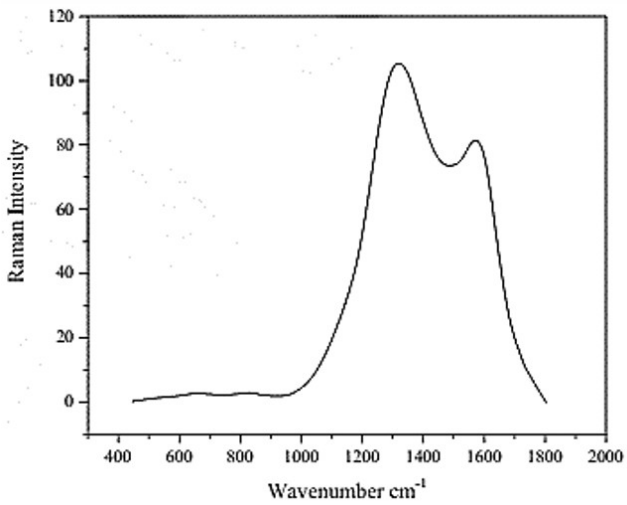

Fig. S9. Raman spectrum of IBOMC

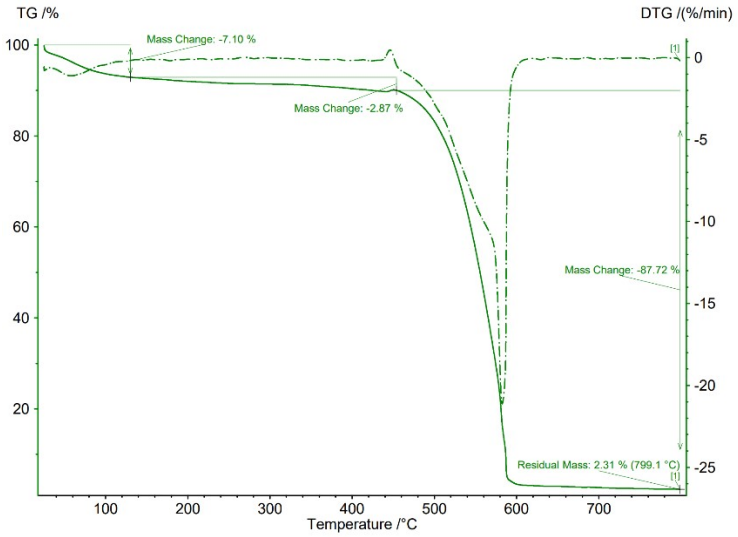

Fig. S10. TGA curve of IBOMC under an O_2 atmosphere

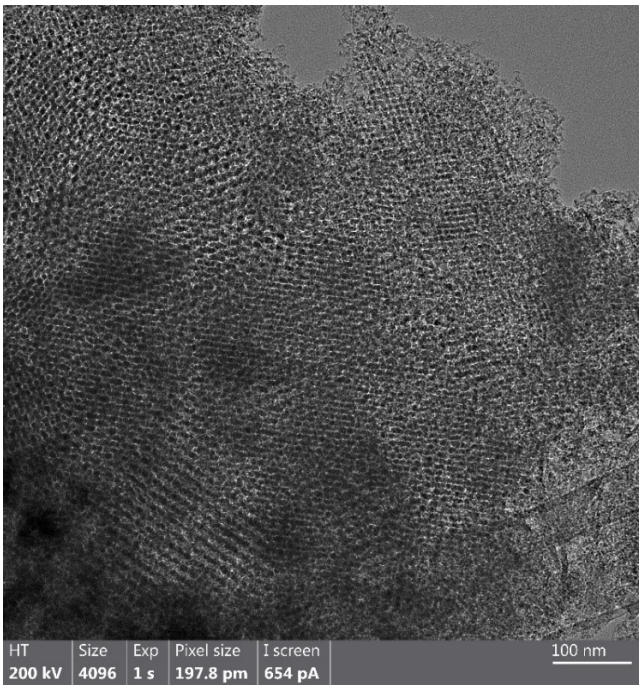

Fig. S11. TEM image of Ru(III)@IBOMC

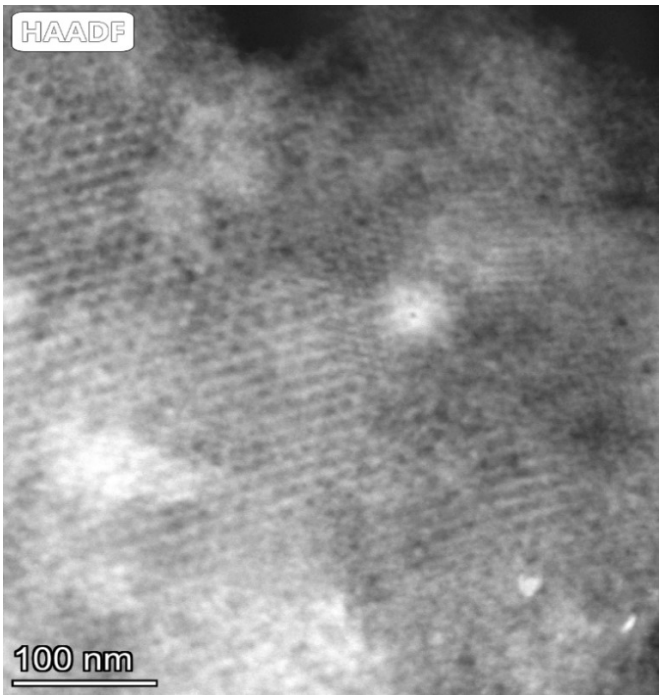

Fig. S12. HAADF-STEM image of Ru(III)@IBOMC

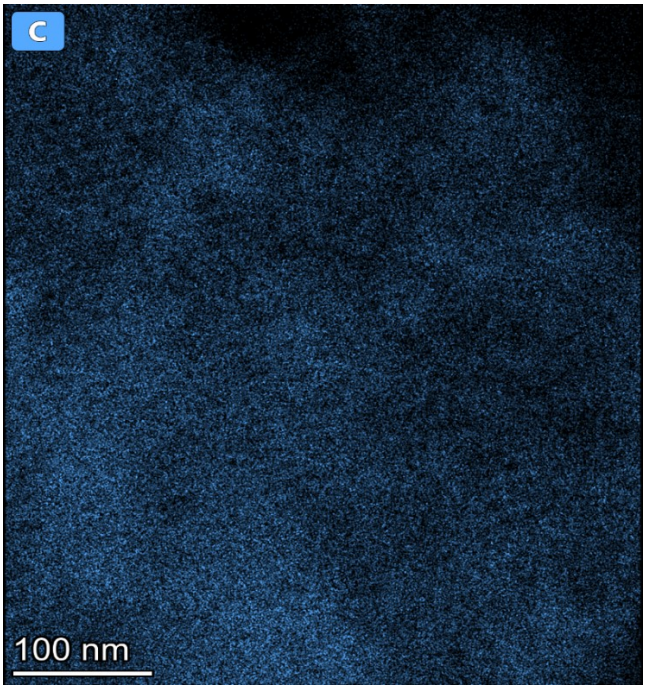

Fig. S13. EDX mapping image for the carbon element of Ru(III)@IBOMC

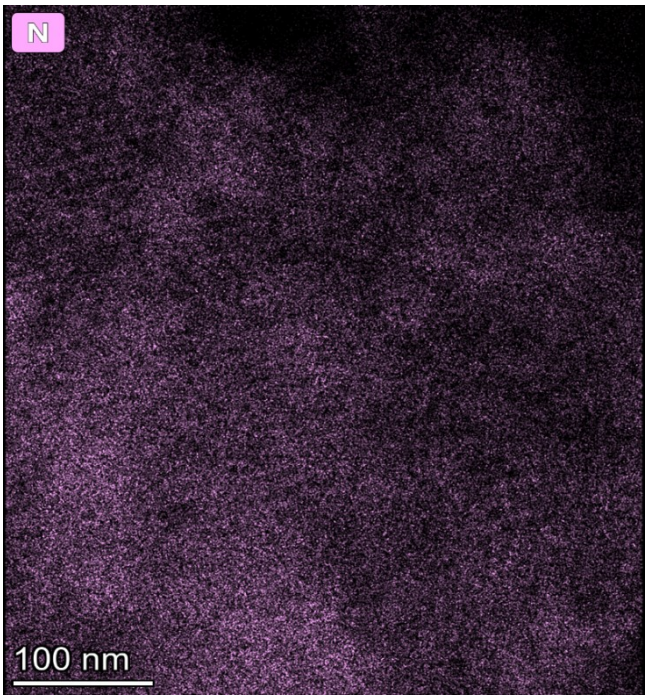

Fig. S14. EDX mapping image for the nitrogen element of Ru(III)@IBOMC

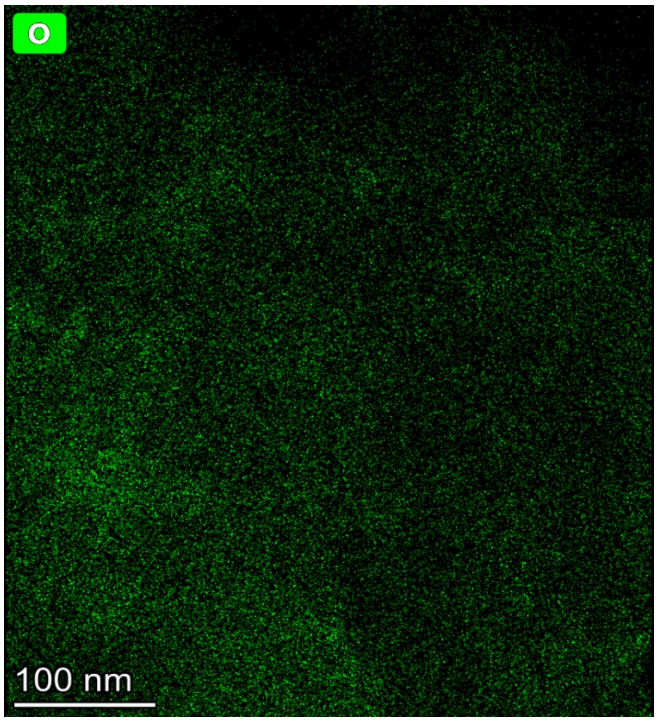

Fig. S15. EDX mapping image for the oxygen element of Ru(III)@IBOMC

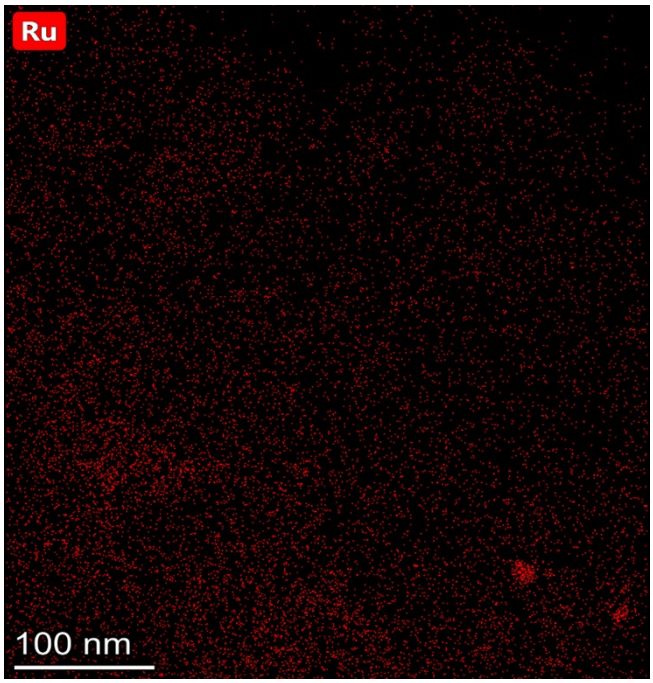

Fig. S16. EDX mapping image for the ruthenium element of Ru(III)@IBOMC

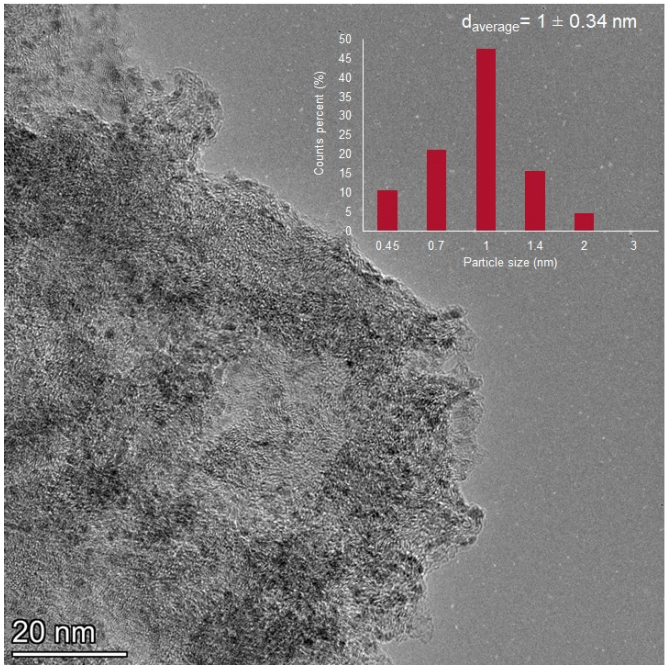

Fig. S17. HRTEM image of Ru(III)@IBOMC (scale bar = 20 nm) and particle size distribution (inset, 352 particles were counted to draw the histogram.) Formulas for calculating daverage and standard deviation:

$$d\ average = \frac{\sum_{i=1}^{n}(F_i \times d_i)}{\sum_{i=1}^{n}(F_i)},$$

$$\sigma = \sqrt{\frac{\sum_{i=1}^{n} F_i(d_i - d_{average})^2}{\sum_{i=1}^{n}(F_i) - 1}}$$

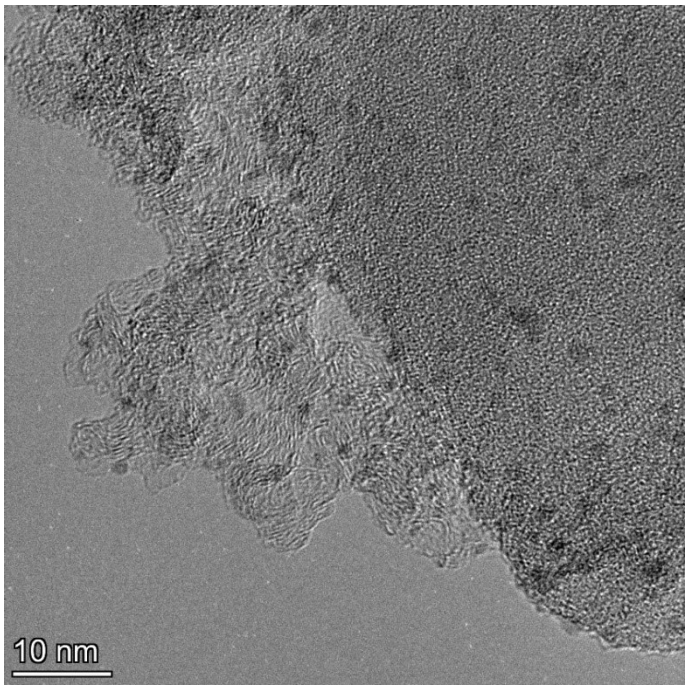

Fig. S18. HRTEM image of Ru(III)@IBOMC (scale bar = 10 nm)

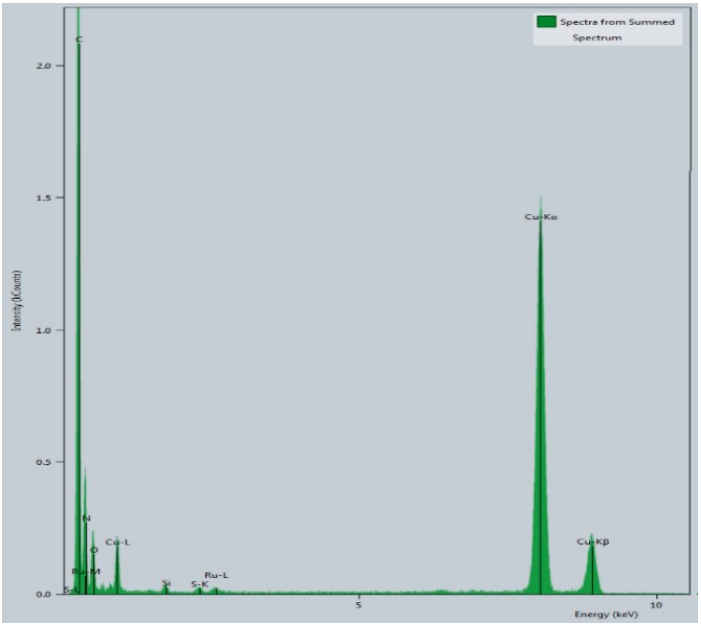

Fig. S19. EDS spectrum of Ru(III)@IBOMC

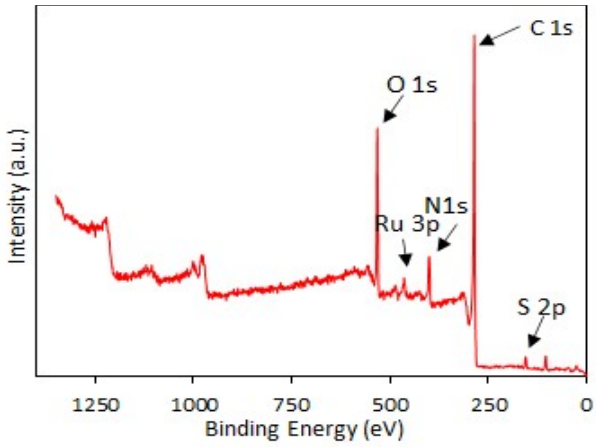

Fig. S20. XPS survey spectrum of Ru(III)@IBOMC

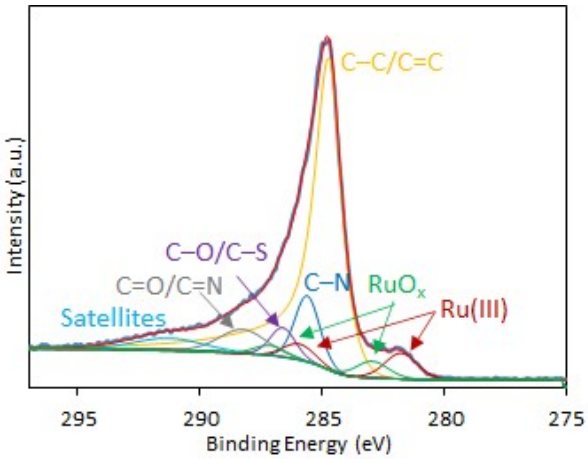

Fig. S21. Deconvoluted C 1s-Ru 3d XPS spectrum of Ru(III)@IBOMC

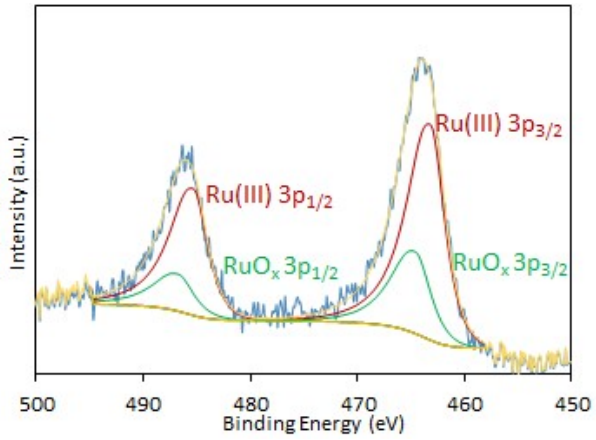

Fig. S 22. Deconvoluted Ru 3p XPS spectrum of Ru(III)@IBOMC

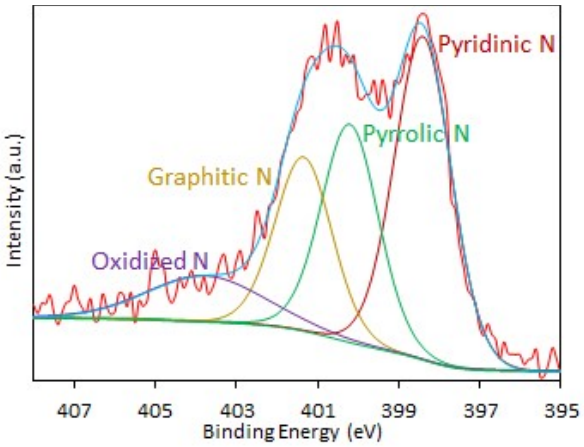

Fig. S23. Deconvoluted N 1s XPS spectrum of Ru(III)@IBOMC

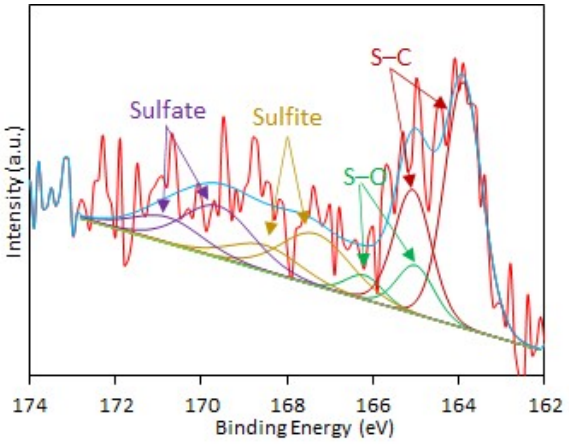

Fig. S24. Deconvoluted S 2p XPS spectrum of Ru(III)@IBOMC

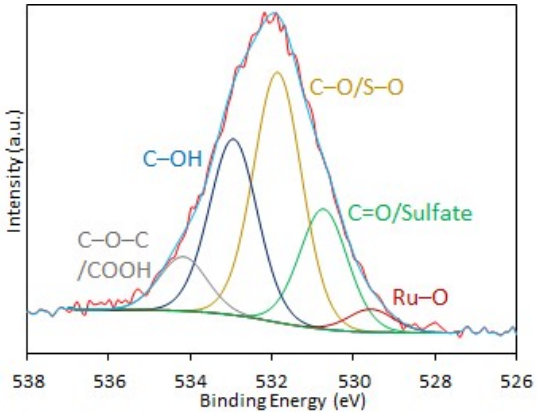

Fig. S25. Deconvoluted O 1s XPS spectrum of Ru(III)@IBOMC

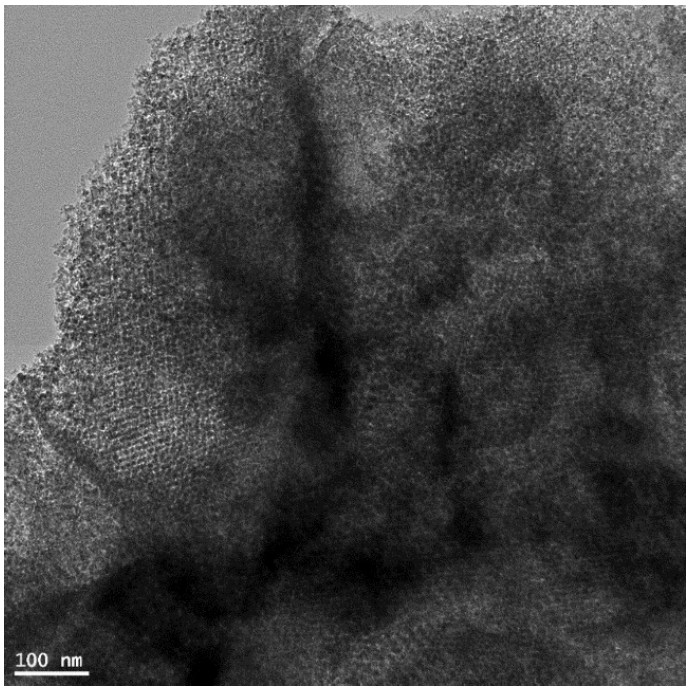

Fig. S26. TEM image of recovered Ru(III)@IBOMC (scale bar = 100 nm)

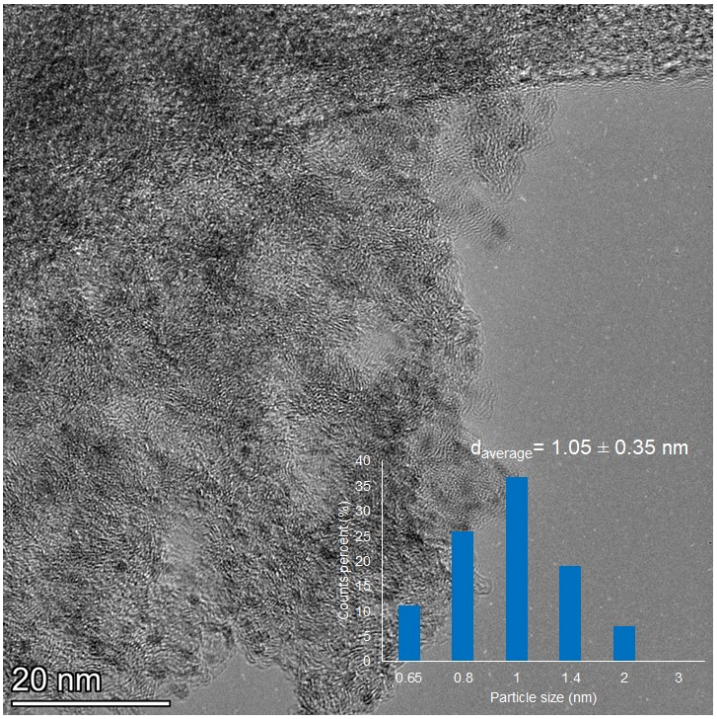

Fig. S27. HRTEM image of recovered Ru(III)@IBOMC (scale bar = 20 nm) and particle size distribution (inset, 382 particles were counted to draw the histogram.) Formulas for calculating daverage and standard deviation:

$$d\ average = \frac{\sum_{i=1}^{n}(F_i \times d_i)}{\sum_{i=1}^{n}(F_i)},$$

$$\sigma = \sqrt{\frac{\sum_{i=1}^{n} F_i(d_i - d_{average})^2}{\sum_{i=1}^{n}(F_i) - 1}}$$

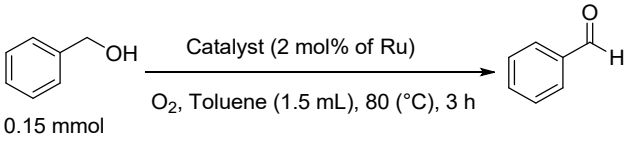

0.15 mmol

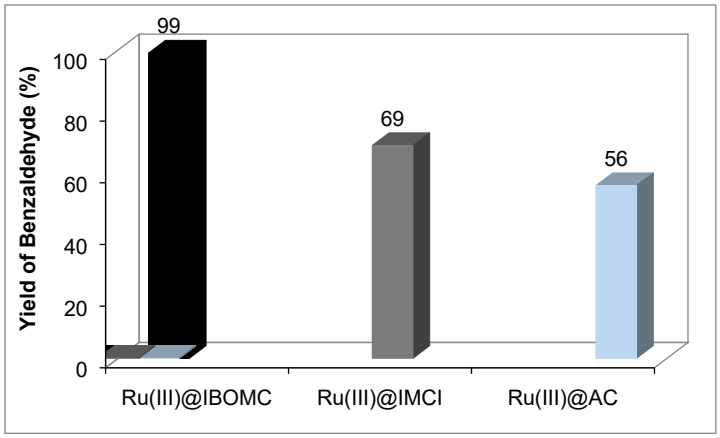

Fig. S28. Comparing the activity of Ru-based catalysts in the oxidation of benzyl alcohol

Table S1. The optimization of the oxidation reaction of benzylamine using the Ru(III)@IBOMC catalyst

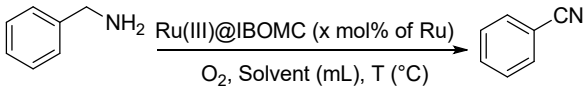

0.15 mmol

Entry	x (mol % of Ru)	Solvent (mL)	T (°C)	Time (h)	Conversion (%)[a]	Selectivity (%)[a]
1	2	Toluene (1.5)	80	3	>99	53
2	2	H_2O (1.5)	80	3	>99	20
3	2	Absolute toluene (1.5)	80	3	>99	>99
4	1	Absolute toluene (1.5)	80	3	63	>99
5	2	Absolute toluene (1)	80	3	88	>99
6	2	Absolute toluene (0.5)	80	3	49	>99
7	2	Absolute toluene (1.5)	90	3	>99	88
8	2	Absolute toluene (1.5)	90	2	>99	93
9	**2**	**Absolute toluene (1.5)**	**80**	**2.5**	**>99**	**>99**
10	2	Absolute toluene (1.5)	80	2	86	>99
11	2	Absolute toluene (1.5)	80	1	49	>99
12[b]	2	Absolute toluene (1.5)	80	2.5	15	>99
13[c]	-	Absolute toluene (1.5)	80	2.5	0	-

[d]The conversion and selectivity were obtained by GC analysis; [b]Ru(III)@activated carbon (2 mol% of Ru, 15 mg) was used as catalyst; [c]IBOMC (20 mg) was used as catalyst.

Table S2. Comparison of several Ru-based heterogeneous catalytic systems used for the aerobic oxidation of alcohols to aldehydes and ketones

Entry	Catalyst (mol %)	Reaction conditions	Type of alcohols	Reusability	Ref.
1	Ru/Al_2O_3 (2.5 mol%)	TFT (1.5 mL), O_2 (1 atm), 85 °C	Primary/secondary benzylic and aliphatic alcohols (18 substrates)	7 cycles	[8]
2	10% Ru/C (5 mol%)	Toluene, O_2 (1 atm), 50-70 °C	Primary/secondary benzylic alcohols, and secondary aliphatic alcohols (18 substrates)	Not done	[9]
3	Ru/CNTs (5.9 mol%)	Toluene (10 mL), H_2O (5 mL), O_2 (0.1 MPa), 85 °C	Primary/secondary benzylic and aliphatic alcohols (12 substrates)	4 cycles	[10]
4	Ru@PMO-IL (2.5 mol%)	TFT (2 mL), O_2 (1 atm), 70 °C	Primary/secondary benzylic and aliphatic alcohols (24 substrates)	5 cycles	[11]
5	rGO@Ru-RM$^{\beta}$-CD[a] (2 mol%)	K_2CO_3 (0.5 mmol), H_2O (4 mL), O_2 balloon, 85 °C	Primary/secondary benzylic and propargylic alcohols (25 substrates)	5 cycles	[12]
6	Ru@OMC (0.8 %)	EtOH, O_2 (1bar), 80 °C	Only benzyl alcohol	4 cycles	[13]
7	Small size non-supported colloidal Ru nanoparticles (0.7 mol%, 20 mg for 3 g substrate)	S.F. or EtOH, O_2 (10 bar), 100 °C	aliphatic, unsaturated and aromatic alcohols (12 substrates)	Not done	[14]
8	Ru@AAO (100 mg, 2.3 wt % Ru)	Toluene (3 mL), air flow (1 atm), 50 °C	Primary/secondary benzylic and aliphatic alcohols (18 substrates)	5 cycles	[15]
9	Ru single atoms anchored onto a nitrogen-doped carbon (Ru_1/NC), (0.31 wt% of Ru, 40 mg)	H_2O, O_2, 90 °C	Primary/secondary and heterocyclic benzylic alcohols, and allylic alcohols (15 substrates)	8 cycles	[16]
10	**Ru(III)IBOMC (2 mol%)**	**Toluene (1.5 mL), O_2 (1 atm), 80 °C**	**Primary/secondary benzylic and aliphatic alcohols (41 substrates)**	**7 cycles**	**This work**

[a]Ruthenium nanoparticles on cyclodextrins modified graphene oxides

Table S3. Comparison of several Ru-based heterogeneous catalytic systems used for the aerobic oxidation of amines to nitriles

Entry	Catalyst (mol	Reaction conditions	Type of amines	Reusability	Ref.

	%)				
1	RuHAP (16.9 mol%, 0.1 g)	Toluene (10 mL), O_2 (1 atm), 110 °C	Primary benzylic and aliphatic amines (15 substrates)	1 cycles	[17]
2	Ru/Al_2O_3 (2.8 mol%)	TFT (5 mL), O_2 (1 atm), 100 °C	Primary benzylic, aliphatic, and heteroatomic amines (11 substrates)	1 cycles	[18]
3	Ru/Co_3O_4 (2.5 mol%)	TFT (5 mL), O_2 flow rate, 100 °C	Primary benzylic, aliphatic, and heteroatomic amines (7 substrates)	5 cycles	[19]
4	5%Ru/AC (3 mol %)	Toluene (5 mL), O_2 (0.5 MPa), 150 °C	Primary benzylic, aliphatic, and heteroatomic amines (15 substrates)	×	[20]
5	Ru@PMO-IL (2.5 mol%)	Anhydrous toluene (2mL), O_2 (1 atm), 85 °C	Primary benzylic, aliphatic and cyclic Amines (13 substrates)	5 cycles	[21]
6	Ru@AAO (125 mg, 2.3 wt % Ru)	Toluene (3 mL), air (1 atm), 90 °C	Primary benzylic, aliphatic, and heteroatomic amines (9 substrates)	5 cycles	[15]
7	$Ru/\gamma\text{-}Al_2O_3$ (7.7 mol%)	Benzotrifluoride (1 mL), O_2 (1 atm), 33 °C, xenon lamp	Primary and secondary benzylic and aliphatic amines (10 substrates)	Not done	[22]
8	$Ru–K–ZrO_2$ (0.7 mol%, 100 mg)	Chlorobenzene (5 mL), O_2 (1.0 MPa), 120 °C,	Primary benzylic, aliphatic, and heteroatomic amines (10 substrates)	Not done	[23]
9	polystyrene-stabilized Ru(III) nanoparticles (PS-Ru(III)NPs) (2.5 mol%)	H_2O, O_2 (1 atm), 50 °C	Primary benzylic and aliphatic amines (8 substrates)	×	[24]
10	**Ru(III)IBOMC (2 mol%)**	**Absolute toluene (1.5 mL), O_2 (1 atm), 80 °C**	**Primary benzylic, aliphatic, and heteroatomic amines (10 substrates)**	**7 cycles**	**This work**

REFERENCES

1 F. Kleitz, S.H. Choi and R. Ryoo, *Chem. Commun*., 2003, 2136.
2 B. Karimi, H. Behzadnia, M. Bostani and H. Vali, *Chem. Eur. J*., 2012, **18**, 8634.
3 H.H. Veisi, M. Akbari, B. Karimi, H. Vali and R. Luque, *Green Chem*., 2023, **25**, 4076.
4 K.S. Weddle, J.D. Aiken and R.G. Finke, *J. Am. Chem. Soc.,* 1998, **20**, 5653.
5 A.P. Umpierre, E. de Jesus and J. Dupont, *ChemCatChem*, 2011, **3***,* 1413.
6 A. Borodziński and M. Bonarowska, *Langmuir*, 1997, **13**, 5613.

7 D. Farin and D. Avnir, *J. Catal.* 1989, **120**, 55.
8 K. Yamaguchi and N. Mizuno, *Angew. Chem., Int. Ed*., 2002, **41**, 4538.
9 S. Mori, M. Takubo, K. Makida, T. Yanase, S. Aoyagi, T. Maegawa, Y. Monguchi and H. Sajiki, *Chem. Commun*., 2009, 5159.
10 X. Yang, X. Wang and J. Qiu, *Appl. Catal. A: Gen.*, 2010, **382**, 131.
11 B. Karimi, D. Elhamifar, O. Yari, M. Khorasani, H. Vali, J. H. Clark and A. J. Hunt, *Chem. Eur. J*., 2012, **18**, 13520.
12 M. R. Patil, A. R. Kapdi and A. Vijay Kumar, *ACS Sustain. Chem. Eng*., 2018, **6**, 3264.
13 L. Wang, J. Zhao, P. Zhang, S. Yang, W. Zhan and S. Dai, *Chem. Eur. J*., 2019, **25**, 8494.
14 J. Zhao, W.Y. Hernández, W. Zhou, Y. Yang, E.I. Vovk, M. Capron and V. Ordomsky, *ChemCatChem*, 2020, **12**, 238.
15 M. A. Hussain, M. Irshad, E.U. Haq, S. Park, M. Atif, A. S. Hakeem, B. G. Choi and J. W. Kim, *Ind. Eng. Chem. Res*., 2019, **58**, 23025.
16 X. Dong, Y. Jia, M. Zhang, S. Ji, L. Leng, J.H. Horton, C. Xu, C. He, Q. Tan, J. Zhang and Z. Li, *Chem. Eng. J.*, 2023, **451**, 138660.
17 K. Mori, K. Yamaguchi, T. Mizugaki, K. Ebitani and K. Kaneda, *Chem. Commun*., 2001, 461.
18 K. Yamaguchi and N. Mizuno, *Angew. Chem., Int. Ed*., 2003, **42**, 1480.
19 F. Li, J. Chen, Q. Zhang and Y. Wang, *Green Chem*., 2008, **10**, 553.
20 B. Niu, F. Lu, H. Y. Zhang, Y. Zhang and J. Zhao, *Chem. Lett*., 2017, **46**, 330.
21 B. Karimi, O. Yari, M. Khorasani, H. Vali and F. Mansouri, *ChemCatChem*, 2018, **10**, 1783.
22 P. Zhu, J. Zhang, J. Wang, P. Kong, Y. Wang and Z. Zheng, Catal. Sci. Technol. 2020, **10**, 440.
23 G. Zhu, S. Shi, X. Feng, L. Zhao, Y. Wang, J. Cao, J. Gao and J. Xu, *ACS Appl. Mater, Interfaces*, 2022, **14,** 52758.
24 M. Kawase, R. Suzuki, K. Kobayashi, T. Shinagawa, A. Tazawa, Y. Uozumi, Y. Matsumura, O. Shimomura and A. Ohtaka, *Chem. Lett.,* 2023, **52**, 553.